Journal of Materials Chemistry C

Influence of the aryl spacer in 2,5-dialkoxyphenylene and diaryl substituted thieno[3,4-c]pyrrole-4,6-dione copolymers

Journal:	*Journal of Materials Chemistry C*
Manuscript ID	TC-ART-02-2018-000823.R1
Article Type:	Paper
Date Submitted by the Author:	23-Apr-2018
Complete List of Authors:	Pankow, Robert; University of Southern California, Chemistry Munteanu, John; University of Southern California, Chemistry Thompson, Barry; University of Southern California, Chemistry

SCHOLARONE™
Manuscripts

Journal Name

ARTICLE

Influence of the aryl spacer in 2,5-dialkoxyphenylene and diaryl substituted thieno[3,4-c]pyrrole-4,6-dione copolymers

Robert M. Pankow[a], John D. Munteanu[a], Barry C. Thompson[a,*]

Received 00th January 20xx,
Accepted 00th January 20xx

DOI: 10.1039/x0xx00000x

www.rsc.org/

Polymerization conditions for direct arylation polymerization (DArP) now allow for the preparation of conjugated polymers, such as donor-acceptor copolymers, where undesired couplings (donor-donor, acceptor-acceptor, or branching defects) are undetectable. This allows for the pursuit of more complex polymer architectures with multiple sites for potential C-H activation, which were previously avoided. Using these conditions, a series of 2,5-dialkoxyphenylene and diaryl substituted thieno[3,4-c]pyrrole-4,6-dione (TPD) copolymers were prepared in order to study the effect of the aryl substituents on the polymer bulk-heterojunction solar cell performance using $PC_{61}BM$ as the acceptor. A material design methodology is investigated, where distancing the sterically incumbered phenylene donor from the TPD acceptor using an aryl spacer is shown to provide improved solar cell performance. The aryl groups incorporated on TPD include bithiophene (BT), thienothiophene (TT), thienylene-vinylene-thienylene (TVT), and ethylenedioxythiophene (EDOT). The BT based copolymer was shown to have the highest performance with a short-circuit current (Jsc) of 10.54 mA cm^{-2}, an open-circuit voltage (Voc) of 0.74 V, and a fill-factor (FF) of 0.61 affording a power conversion efficiency of 4.76%, which is the highest reported efficiency for a 2,5-dialkoxy phenylene copolymer prepared using DArP to the best of our knowledge.

Introduction

Through the optimization of the polymerization conditions and the careful selection of substrates, direct arylation polymerization (DArP) has begun to provide polymeric materials equivalent to or surpassing those prepared using traditional transition metal-catalyzed cross-coupling methods, in terms of photovoltaic (PV) device performance.[1–6] Architectures have progressed from homopolymers to perfectly alternating donor-acceptor copolymers and towards even more complex semi-random and random architectures.[2,7–18] Through modification of the polymerization conditions employed, e.g. changing the ligands for the palladium catalyst or the carboxylic acid additive, DArP conditions originally reported by Ozawa et al. have been optimized to provide conjugated polymer products with undetectable levels of homocoupling (either donor-donor or acceptor-acceptor) and branching (β) defects.[7,19–26] In our previous works, this has allowed for the preparation of the perfectly alternating donor-acceptor copolymers and random copolymers shown in **Figure 1**,[7,19] with the corresponding molecular weights (M_n) and power conversion efficiencies (PCE) for PV devices provided for pol[2,5-bis(2hexyldecyloxy)phenylene-alt-(4,7-dithiophen-2-yl)benzo[c][1,2,5]thiazole)] (PPDTBT), pol[2,5-bis(2hexyldecyloxy)phenylene-alt-(5-octyl-1,3-di-2-thienyl-thieno[3,4-c]pyrrole-4,6-dione)] (PPDTTPD) and poly[(2,5-bis[(hexyloxy)phenylene])-alt-(5-octyl-1,3-di-2-thienyl-thieno[3,4-c]pyrrole-4,6-dione)-alt-(2,5-bis[(2-hexyldecyl)oxyphenylene])] r-(PPDTTPD).

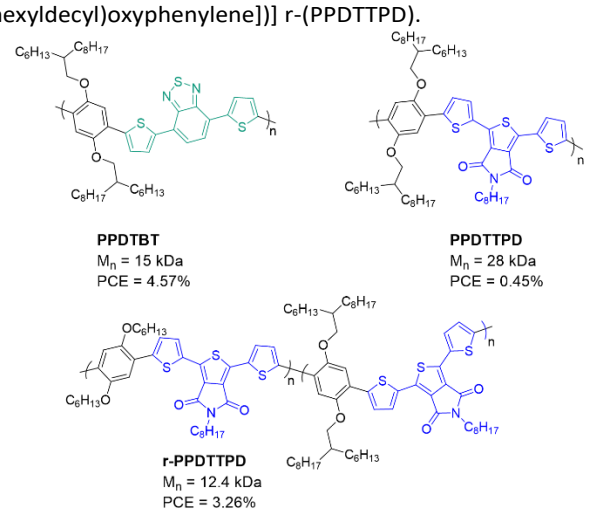

Figure 1. M_n and PCE for the polymers PPDTBT (15 kDa, 4.57%), PPDTTPD (28 kDa, 0.45%), and r-PPDTTPD (12.4 kDa, 3.26%), respectively, which were prepared previously using optimized DArP conditions.

Recently, PPDTBT prepared using DArP in a continuous flow process provided a PCE of 3.5% when incorporated into a roll-to-roll (R2R) printed PV device.[27] The phenylene donor and dithienylbenzodithiazole (DTBT) acceptor used for this polymer can be prepared in a few facile, scalable steps making the starting materials for this polymer easily accessible in large quantities. PPDTBT also displays good environmental stability, as evidenced by PV device fabrication and testing under

[a] Department of Chemistry and Loker Hydrocarbon Research Institute, University of Southern California, Los Angeles, California 90089-1661. *Email: barrycth@usc.edu

Electronic Supplementary Information (ESI) available: [Monomer synthesis and characterization, Polymer synthesis and characterization, DSC, CV, XRD, NMR, PV device, and EQE data.]. See DOI: 10.1039/x0xx00000x

Please do not adjust margins

ambient conditions. Given these factors, PPDTBT displays all the outstanding merits needed to make organic photovoltaics (OPV) a competitive technology, including: a small number of easily achieved synthetic steps and good performance in large-area, R2R processed devices fabricated and tested under ambient conditions. These attributes enable taking solar-cells out of the glovebox to under the sun, motivating the quest to find polymers with similar attributes.[19,28–31]

Towards this goal, PPDTTPD was investigated because thieno[3,4-c]pyrrole-4,6-dione (TPD) possesses many of the same qualities as its DTBT counterpart, e.g. small number of facile, scalable synthetic steps, desirable optical and electronic properties when incorporated into a conjugated polymer, and good performance in PV devices. However, the polymer PPDTTPD required modification via incorporation of a second phenylene donor with shorter, linear alkyl chains to provide satisfactory PV device performance (r-PPDTTPD, **Fig. 1**). The improved PV device performance is attributed to the hypothesis that minimizing alkyl-chain congestion near the acceptor unit will allow for improved interaction with the fullerene, thereby increasing the values for J_{SC} and fill factor (*FF*). [32–36] Unlike PPDTTPD, it is believed that PPDTBT allows for improved fullerene interactions due to the absence of alkyl chains directly attached to the DTBT acceptor moiety. Due to the alkyl chains on TPD, it seems that alkyl chain congestion of the acceptor moiety is exacerbated and must otherwise be minimized. With this design principle in mind, distancing the TPD acceptor from the sterically incumbered phenylene donor through the implementation of an aryl spacer moiety with an extended π-system may allow for the preparation of polymers that possess properties closer to that of PPDTBT.

To support this claim, it has been shown that TPD copolymers incorporating donors with extended conjugation can provide enhancements in short-circuit current (J_{SC}) densities, while maintaining the high-values for open-circuit voltage (V_{OC}) characteristic of many TPD based copolymers.[37–41] However, this methodology has not been explicitly applied to 2,5-dialkoxyphenylene copolymers, to our knowledge. Such extended spacers that do not bear sterically demanding alkyl solubilizing groups will invariably contain multiple aryl C-H sites that are potentially reactive in DArP. Since a condition set that minimizes all defects to undetectable levels has been realized, we were emboldened to incorporate monomers with a high-population of sites for C-H activation that also provide extended conjugation. In this way we seek to address the challenge of TPD-based dialkoxypheneyle copolymers, while simultaneously probing the capacity of DArP.

Herein, we report the synthesis and characterization of dialkoxy phenylene and diaryl TPD copolymers, where the aryl group is varied in pursuit of optimal PV device performance. The specific motivation being to discern if an aryl unit that provides extended conjugation can improve the device performance relative to PPDTTPD. Illustrated in Scheme 1, we selected bi-thiophene (BT), thienothiophene (TT), and thienylenevinylenethienylene (TVT).[2,42–44] The strong donor, ethylene dioxy thiophene (EDOT), was also chosen to demonstrate that improved material device performance is a result of extending the conjugation and improving polymer/fullerene interaction, rather than just inclusion of a stronger donor, which BT, TT, and TVT provide as well.

Results and Discussion

The polymers in Scheme 1 were prepared using optimized DArP conditions we have shown[7,19] to provide polymer products with undetectable homocoupling and β-defects through the inclusion of a bulky carboxylic acid additive, such as neo-decanoic acid (NDA) (where NMR, UV-vis spectroscopy, and photovoltaic device performance have been used to directly or indirectly confirm or exclude the presence of these defects).[1,16,45] Based initially on the pioneering work of Ozawa et al.,[22] which was further expanded upon by Leclerc et al.,[20,23] these conditions provide exceptional polymer products incorporating a wide variety of monomers.[46] Illustrated in Scheme 1, these conditions employ Pd_2dba_3 as the palladium source, P(o-anisyl)$_3$ as a phosphine ligand, Cs_2CO_3 as a base, NDA as a carboxylic acid additive, and superheated tetrahydrofuran (THF) as the solvent. The polymerizations were executed in a sealed, high-pressure vessel under a nitrogen atmosphere. Detailed experimental info, including monomer syntheses can be found in the electronic supporting info (ESI).

Structural and electronic characterization for polymers **P1**-**P4** including molecular weights (M_n), melt and crystallization-transition temperatures (T_m and T_c), d_{100} spacing, electrochemical HOMO values, absorbance maxima (λ_{max}), absorption coefficients (α), and SCLC hole mobilities (μ_h) are all provided in **Table 1**. In regards to molecular weights (M_n), polymer P1 displays the highest at 16.5 kDa. Issues with solubility are likely the cause of low M_n observed for polymer P2 (3.90 kDa), P3 (7.47 kDa), and P4 (9.02 kDa) leading to polymer products precipitating out of the reaction mixture prematurely. The TPD monomers themselves for P3 and P4 possess especially low solubility. However, all polymeric materials recovered from the reaction mixture were capable of dissolving in hot, chlorinated solvents, and no insoluble material was observed in the thimble after Soxhlet with $CHCl_3$. The diminished solubility is a perceived consequence of introducing a more rigid π-system via the aryl substituent of TPD, relative to the previously used 2-thienyl for PPDTTPD shown in Figure 1. Improving the molecular weight can likely be accomplished for P2-P4 by incorporating a more powerful solubilizing chain on the TPD unit, but that may diminish fullerene interaction with the

This journal is © The Royal Society of Chemistry 20xx

Please do not adjust margins

Scheme 1. Preparation of Polymers P1-P4 using DArP.

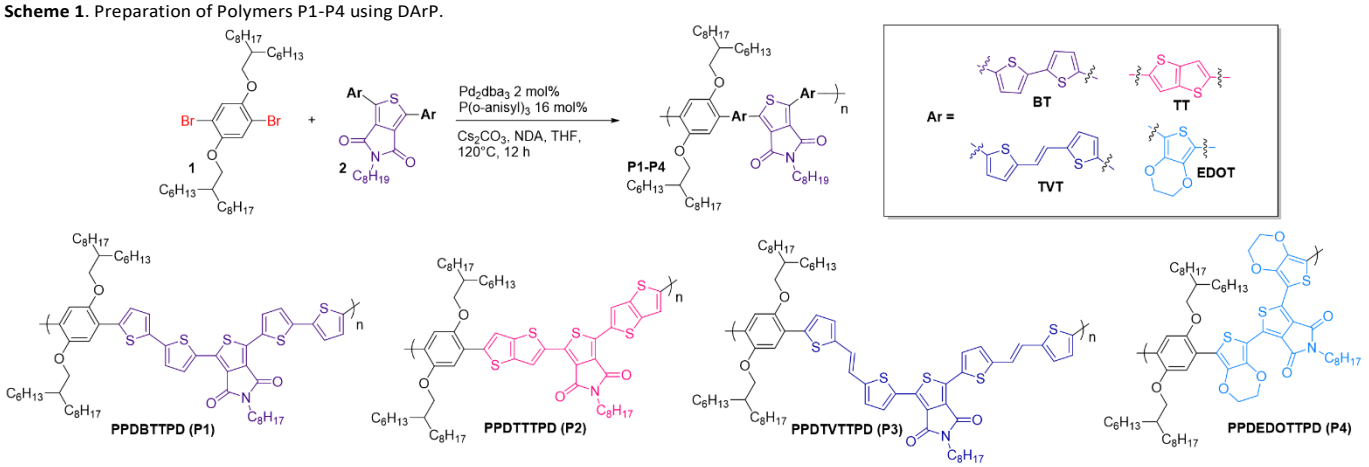

Table 1. Molecular Weights (*Đ*), Melt and Crystallization Temperatures (T_m and T_c), d_{100} spacing, Electrochemical HOMO Values, and SCLC Hole Mobilities (μ_h) of Polymers P1-P4.

Entry	M_n *(kDa); Đ*[a]	T_m; T_c *(°C)*[b]	d_{100} *(Å)*[c]	*HOMO (eV)*[d]	λ_{max} *(nm)*[e]; α *(cm*$^{-1}$*)*[e]	μ_h (cm^2 V^{-1} sec^{-1})
P1	16.5; 2.1	319; 301	22.4	-5.59	620; 7.26 × 10^4	2.95 × 10^{-4}
P2	3.9; 1.7	316; 295	19.4	-5.46	583; 7.07 × 10^4	5.02 × 10^{-7}
P3	7.5; 2.1	302; 295	20.7	-5.44	577; 6.63 × 10^4	9.52 × 10^{-5}
P4	9.0; 1.5	336; 319	-	-5.05	571; 3.87 × 10^4	4.73 × 10^{-5}

[a]As determined by SEC calibrated by polystyrene standards after Soxhlet extraction. [b]Determined by DSC. [c]Calculated from GIXRD peaks of thin films. [d]Determined from E_{ox} onset using cyclic voltammetry of polymer films using Fc/Fc$^+$ as an internal reference in MeCN with 0.1 M TBAPF. [e]Determined from polymer films.

acceptor moiety leading to diminished device performance.[32–36,47] Another route would be to incorporate an unsymmetrical diaryl TPD acceptor, where one of the aryl units is thiophene and the other is either TT or TVT, although this may complicate and prolong the synthetic route. ^{1}H NMR spectra in $CDCl_3$ of the polymers (see ESI) contain broad, featureless aromatic regions characteristic of many known TPD incorporated polymers.[7,38,48] However, donor-donor homocoupling defects appear absent (δ7.10 ppm), and equal incorporation of the donor unit and TPD can be verified through relative integrations of the alkyl chains on the phenylene donor and TPD acceptor (δ5.00-3.50 ppm). This indirectly provides evidence for the absence or minimization of acceptor-acceptor homocouplings to undetectable levels.[49] Also, high-temperature ^{1}H NMR experiments (100 °C) in $C_2D_2Cl_4$ were performed to confirm the polymer structure, and those spectra are provided in the ESI. While β-defects are challenging to interpret using ^{1}H NMR, except for well-studied and simpler systems such as poly(3-hexylthiophene) (P3HT), the exclusion or minimization can be realized using indirect methods such as UV-vis spectroscopy, PV device characterization, and the absence of insoluble materials after polymer purification, as mentioned previously.[15,21,25,26,43,50–54]

The polymers all display semi-crystallinity (albeit low degrees of crystallinity, see ESI), as shown with the T_m and T_c values provided in Table 1. The thermal properties are all quite similar with thermal transitions in excess of 300 °C. It is worth noting the thermal transitions for P4 are the highest reported, to our knowledge, for any phenylene and TPD based copolymer, with a T_m of 336 °C and a T_c of 319 °C. Values for the *d*-spacing (measured via GIXRD) are also similar for the polymers P1-P3 (19.4-22.4 Å), which is reasonable given the alkyl chains on the phenylene donor and the TPD acceptor remain constant for this study. The polymer films were all annealed at 210 °C for 60 min., and despite this semi-crystallinity was not observed for polymer P4 using XRD. This is likely a consequence of the high T_m of the polymer, where annealing conditions were found to be ineffective for inducing semi-crystallinity within thin films.[55]

Please do not adjust margins

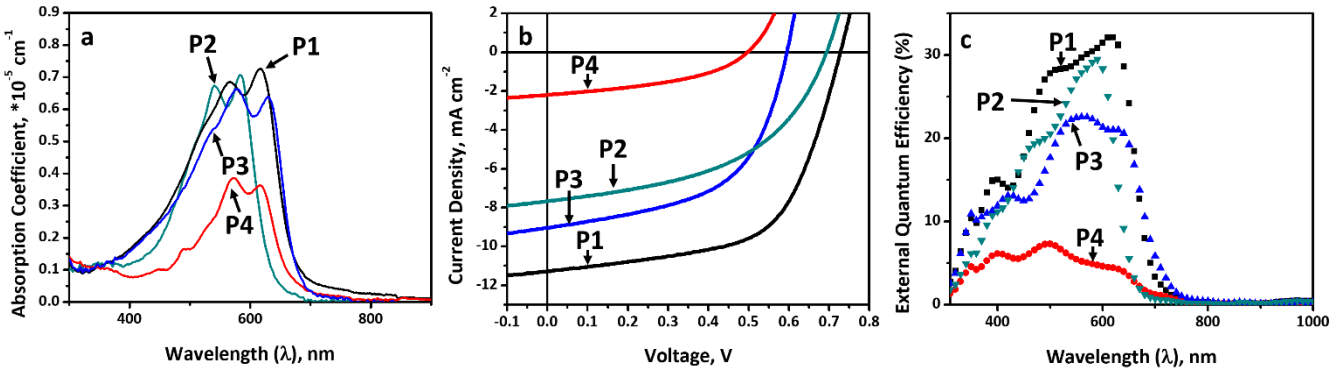

Figure 2. (a) UV-vis absorbance of polymer (**P1**-**P4**) films spin-coated from a 7 mg mL^{-1} DCB solution and annealed at 210 °C for 50 minutes. (b) *J-V* curves of polymers P1-P4. (c) EQE traces of polymers P1-P4.

Table 2. Photovoltaic device performance for polymers P1-P4.

Entry	J_{SC} (mA cm^{-2})[a]	V_{OC} (V)	FF	PCE (%)[b]
P1	10.54	0.74	0.61	4.76
P2	7.59	0.70	0.49	2.60
P3	9.28	0.60	0.52	2.89
P4	2.45	0.49	0.41	0.49

[a]Mismatch corrected. [b]Results are average of at least eight pixels.

Attempts to anneal films of P4 at higher temperatures (250 °C and 300 °C) lead to visible decomposition of the polymer film.

As expected, modification of the aryl groups attached to TPD influence the electronic properties of the polymers. Electrochemical HOMO energy levels (Table 1) increase dependent on the donor-strength of the aryl unit, as apparent when going from BT to EDOT. Where the more rigid, coplanar aryl units, or electron-rich unit in the case of EDOT, provide relatively higher HOMO energy levels. P1, which incorporates BT, possesses the deepest HOMO at -5.59 eV. Alternatively, P4, which incorporates EDOT, possess the highest HOMO at -5.05 eV. Both P2 and P3 possess relatively intermediate and similar HOMO energy levels at -5.46 and -5.44 eV, respectively.

Shown in Table 1 and illustrated in Figure 2a, a dependence on the aryl unit incorporated is observed for polymers P1-P4 in the thin-film absorption. A bathochromic shift is observed for P1, relative to P2-P4, which possesses absorption from approximately 400-700 nm with λ_{max} situated at 620 nm. P3 possesses a similar absorption breadth, however its λ_{max} is shifted to 577 nm. Both P2 and P4 possess narrower absorption profiles from approximately 400-650 and 450-700 nm, with peak absorbance at 583 and 571 nm, respectively. Polymers P1-P3 possess similar values for the absorption coefficient (α) (7.26 × 10^4-6.63 × 10^4 cm^{-1}, respectively) however that for P4 is significantly lower (3.87 × 10^4 cm^{-1}). This is likely due to steric hindrance disrupting packing and organization between polymer chains, limiting the amount or extent of π-π interactions. To that end, a relatively low value for α was previously observed for PPDTTPD, making this result expected.[7]

All polymers show a strong vibronic shoulder, characteristic of polymers with minimized or excluded β-defects.[19,45]

SCLC hole mobilities were determined using the hole-only device architecture ITO/PEDOT:PSS/polymer/Al fabricated and tested under ambient conditions. The polymer layer was spin-casted from a 7 mg ml^{-1} solution in DCB. The obtained mobilities for polymers P1-P4 (Table 1) illustrate a dependence on the molecular weight and aryl spacer used, with P1 displaying the highest value for mobility (2.95 × 10^{-4} cm^2 V^{-1} sec^{-1}). P4 possesses a lower hole-mobility, relative to P1 and P3, which is likely due to the diminished semi-crystallinity of P4 and disrupted π-π interactions from unfavourable steric interactions.[2,56,57] The lowest value for hole mobility was observed for P2 (5.02 × 10^{-7} cm^2 V^{-1} sec^{-1}), which is likely due to the low M_n. Notably, the polymers P1 and P3 display improved hole-mobilities when compared to PPDTBT, r-PPDTTPD, and PPDTTPD (8.81 × 10^{-5}, 3.18 × 10^{-5}, and 2.30 × 10^{-5} cm^2 V^{-1} sec^{-1}, respectively).[7,19]

Photovoltaic (PV) devices were fabricated and tested under ambient conditions, using the conventional architecture ITO/PEDOT:PSS/polymer:PCBM/Al, and device results are provided in **Table 2**. Active layers were spin-casted from 11 mg mL^{-1} solutions of polymer:PC$_{61}$BM mixtures in DCB, and polymer to PC$_{61}$BM ratios are 1:1.5. Polymers P1-P3, which incorporate aryl spacers with extended conjugation, all provided higher PCE relative to PPDTTPD (Figure 1, 0.45%). Polymer P1 displays the most desirable values for J_{sc} (10.54 mA cm^{-2}), V_{oc} (0.74 V), and *FF* (0.61). Polymers P2 and P3 displayed similar values for PCE at 2.60% and 2.89%, respectively. The good fill-factors obtained for P1-P3 are characteristic of minimized or excluded β-defects.[45] The lower efficiencies obtained for P2 and P3, relative to P1, is at least partially due to the low M_n for these polymers.[56,57] The lower solubility of these polymers made device fabrication a challenging endeavor, although acceptable results were obtained when processed in hot DCB (110 °C). Polymer P4 provided a low efficiency of 0.49% very similar to PPDTTPD. This is likely consequential of the hindered polymer-fullerene interactions and the observation that many polymers incorporating EDOT have struggled to provide relatively high efficiencies, at least with a conventional device architecture.[2,58] As originally envisioned, the polymers

This journal is © The Royal Society of Chemistry 20xx

Please do not adjust margins

(P1-P3) with π-extended spacers all provide improved values for J_{sc} and *FF* relative to PPDTTPD. Adjustments in values for V_{oc} can be correlated to the differences in the respective HOMO energy levels for each polymer, with the exception of P3.[59] Specifically, the lowest value for V_{oc} was obtained with P4 which possess the highest HOMO energy level, while P1 which possesses the deepest HOMO energy level provides the highest value for V_{oc}. It appears as if the optimal device results obtained for P1 are due to an achieved balance between processability and better intermolecular interactions with the fullerene acceptor, similar to what is observed with PPDTBT.[31] Thus, P1 provides an improved device results to that of PPDTBT. EQE data (Figure 2c) corroborates the trend observed with increasing J_{sc} values for polymers P1-P4. With the EQE_{max} for P1, P2, P3, and P4 at 32% (616 nm), 29% (590 nm), 22% (561 nm), and 7% (498 nm), respectively. The PCE obtained for P1 makes this an excellent candidate for future studies in large area, roll-coated devices.

Experimental

General Procedure for the Preparation of Polymers P1-P4.

An oven dried 15 mL high pressure vessel was cooled under a stream of N_2. Then neodecanoic acid (0.5 mmol), **1** (0.25 mmol), **2** (0.25 mmol), P(o-anisyl)$_3$ (16 mol%), $CsCO_3$ (3 equiv.), and freshly distilled THF (2.5 mL) were added to the vessel. It was sparged with N_2 for 15 minutes, then Pd_2dba_3 (2 mol%) was added quickly, and the Teflon screwcap with o-ring was fastened tightly. It was then placed in a preheated oil bath at 120 °C for 12 hr. The vessel was then cooled, the contents dissolved in chlorinated solvents ($CHCl_3$ or chlorobenzene), and then the polymer was precipitated slowly via pipette to cold MeOH and allowed to stir for several minutes. The solids were then filtered off into a Soxhlet thimble and extracted with MeOH (24 hr.), hexanes (16 hr.), and then $CHCl_3$. The $CHCl_3$ fraction was concentrated and the polymer precipitated into cold MeOH, filtered off, and dried under vacuum.

Solar Cell Device Fabrication and Characterization.

All steps of device fabrication and testing were performed at ambient temperatures and humidity in air. ITO-coated glass substrates (10 Ω/sq, Thin Film Devices Inc.) were sequentially cleaned by sonication in detergent solution, deionized water, tetrachloroethylene, acetone, and isopropyl alcohol, and dried under a nitrogen stream. PEDOT:PSS (Clevios™ PH 1000, filtered with a 0.45 µm poly(vinylidene fluoride) (PVDF) syringe filter—Pall Life Sciences) was spin-coated on the freshly cleaned ITO-coated glass substrates and then annealed at 120 °C for 50 min under vacuum to generate a 40 nm thick film. Separate solutions of the polymers and $PC_{61}BM$ were prepared in o-DCB. The solutions were stirred for 8 h at 65 °C (P1 and P4) or 110 °C (P2 and P3) before they were mixed to afford a 1:1.5 (polymer:PCBM) ratio and stirred for 16 h at 65 °C (P1 and P4) or 110 °C (P2 and P3) to form a homogeneous solution prior to spin-coating. The polymer:$PC_{61}BM$ active layer was filtered (with a 0.45 µm polytetrafluoroethylene (PTFE) syringe filter—Pall Life Sciences) and spin-coated on top of the PEDOT:PSS layer. Polymer: $PC_{61}BM$ concentrations of the blends were 11 mg/mL respective to the total polymer weight. For consistency across all polymers, every device was kept in a nitrogen box for 25 min after spin-coating and then placed in the vacuum chamber for aluminium deposition. Aluminium was deposited using a Denton Benchtop Turbo IV Coating System. The substrates were pumped down to high vacuum (1.5×10^{-6} torr) and aluminium (100 nm) was thermally evaporated at 3–6 Å/s onto the active layer through shadow masks to define the active area of the devices as 5.18 mm^2. Device results shown are the average of at least 8 pixels. The current density–voltage (J–V) characteristics of the photovoltaic devices were measured under ambient conditions using a Keithley 2400 source-measurement unit. An Oriel® Sol3A class AAA S11 solar simulator with a Xenon lamp (450 W) and an AM 1.5G filter was used as the solar simulator. An Oriel PV reference cell system 91150 V was used as the reference cell to calibrate the light intensity of the solar simulator (to 100 mW/cm^2), achieved by making the J_{sc} of the reference cell under simulated sunlight as high as it was under the calibration condition. External quantum efficiency (EQE) measurements were performed using a 300 W Xenon arc lamp (Newport Oriel), chopped and filtered monochromatic light (250 Hz, 10 nm FWHM) from a Cornerstone 260 1/4 M double grating monochromator (Newport 74125) together with a light bias lock-in amplifier. A silicon photodiode calibrated at Newport was utilized as the reference cell.

Conclusions

In summary, a series of 2,5-dialkoxy phenylene and diaryl-TPD copolymers were prepared using DArP and fully characterized. Structural characterization of the polymers indicates a minimization or exclusion of homocoupling and β-defects, as evidenced by ^{1}H NMR, UV-vis spectroscopy, and the high fill-factors obtained for PV devices. These results show that the DArP conditions used for polymerzation allow for the preparation of conjugated copolymers with a high population of potential C-H activation sites. It was found that the aryl units with extended conjugation (P1, P2, and P3) provided the best PV device efficiencies (4.76%, 2.60%, and 2.89%, respectively) in comparison to thiophene (PPDTTPD) and EDOT (P4) (0.45% and 0.49%, respectively). These results demonstrate support for the hypothesis that providing a π-conjugated spacer between the TPD acceptor and the phenylene donor allow for improved polymer:PCBM interactions, by limiting the steric interactions between the polymer's donor and acceptor moieties. This steric hindrance may potentially impair intermolecular interactions between the acceptor moiety of the polymer and the fullerene leading to a reduction in the PCE of a PV device, which is what was observed for PPDTTPD and P4.[32–36] This methodology can likely be applied to incorporate other acceptors that possess alkyl chains, such as diketopyrrolopyrrole (DPP), qunioxaline, and benzotriazole. Future studies will seek to find an optimal solubilizing chain for the TPD acceptor that may provide improved processability and PV device performance. Also, use of an unsymmetric diaryl-TPD, e.g. one with thiophene and TVT

Please do not adjust margins

aryl units, may allow for improved processability and interesting electronic properties beneficial to photovoltaic devices.

Acknowledgements

This work was supported by the National Science Foundation (MSN under award number CHE-1608891), the Dornsife/Graduate School Fellowship (to R.M.P.), and the Cerritos College Foundation (to J.D.M.).

Notes and references

1 N. S. Gobalasingham, S. Ekiz, R. M. Pankow, F. Livi, E. Bundgaard and B. C. Thompson, *Polym. Chem.*, 2017, **8**, 4393–4402.
2 N. S. Gobalasingham, R. M. Pankow, S. Ekiz and B. C. Thompson, *J. Mater. Chem. A*, 2017, **5**, 14101–14113.
3 S. Kowalski, S. Allard, K. Zilberberg, T. Riedl and U. Scherf, *Progress in Polymer Science*, 2013, **38**, 1805–1814.
4 A. S. Dudnik, T. J. Aldrich, N. D. Eastham, R. P. H. Chang, A. Facchetti and T. J. Marks, *J. Am. Chem. Soc.*, 2016, **138**, 15699–15709.
5 T. Bura, J. T. Blaskovits and M. Leclerc, *J. Am. Chem. Soc.*, 2016, **32**, 10056-10071.
6 T. Bura, S. Beaupre, M.-A. Legare, J. Quinn, E. Rochette, J. T. Blaskovits, F.-G. Fontaine, A. Pron, Y. Li and M. Leclerc, *Chem. Sci.*, 2017, **8**, 3913-3925.
7 R. M. Pankow, N. S. Gobalasingham, J. D. Munteanu and B. C. Thompson, *J. Polym. Sci., Part A: Polym. Chem.*, 2017, **55**, 3370–3380.
8 N. S. Gobalasingham, R. M. Pankow and B. C. Thompson, *Polym. Chem.*, 2017, **8**, 1963–1971.
9 A. E. Rudenko, P. P. Khlyabich and B. C. Thompson, *ACS Macro Lett.*, 2014, **3**, 387–392.
10 A. E. Rudenko, C. A. Wiley, S. M. Stone, J. F. Tannaci and B. C. Thompson, *J. Polym. Sci., Part A: Polym. Chem.*, 2012, **50**, 3691–3697, S3691/1-S3691/19.
11 A. E. Rudenko, P. P. Khlyabich and B. C. Thompson, *J. Polym. Sci., Part A: Polym. Chem.*, 2016, **54**, 1526–1536.
12 J. Kuwabara, N. Takase, T. Yasuda and T. Kanbara, *J. Polym. Sci., Part A: Polym. Chem.*, 2016, **54**, 2337–2345.
13 J. Kuwabara, T. Yasuda, S. J. Choi, W. Lu, K. Yamazaki, S. Kagaya, L. Han and T. Kanbara, *Adv. Funct. Mater.*, 2014, **24**, 3226–3233.
14 J. Kuwabara, Y. Fujie, K. Maruyama, T. Yasuda and T. Kanbara, *Macromolecules (Washington, DC, U. S.)*, 2016, **49**, 9388–9395.
15 T. Bura, P.-O. Morin and M. Leclerc, *Macromolecules*, 2015, **48**, 5614–5620.
16 T. Bura, S. Beaupré, M.-A. Légaré, J. Quinn, E. Rochette, J. T. Blaskovits, F.-G. Fontaine, A. Pron, Y. Li and M. Leclerc, *Chem. Sci.*, 2017, **8**, 3913–3925.
17 T. Bura, J. T. Blaskovits and M. Leclerc, *J. Am. Chem. Soc.*, 2016, **138**, 10056–10071.
18 H. Bohra, S. Y. Tan, J. Shao, C. Yang, A. Efrem, Y. Zhao and M. Wang, *Polym. Chem.*, 2016, **7**, 6413–6421.
19 F. Livi, N. S. Gobalasingham, B. C. Thompson and E. Bundgaard, *J. Polym. Sci., Part A: Polym. Chem.*, 2016, **54**, 2907–2918.
20 C. Roy, T. Bura, S. Beaupré, M.-A. Légaré, J.-P. Sun, I. G. Hill and M. Leclerc, *Macromolecules*, 2017, **50**, 4658–4667.
21 E. Iizuka, M. Wakioka and F. Ozawa, *Macromolecules*, 2016, **49**, 3310–3317.
22 M. Wakioka, Y. Kitano and F. Ozawa, *Macromolecules*, 2013, **46**, 370–374.
23 P.-O. Morin, T. Bura, B. Sun, S. I. Gorelsky, Y. Li and M. Leclerc, *ACS Macro Lett.*, 2015, **4**, 21–24.
24 F. Nübling, H. Komber and M. Sommer, *Macromolecules*, 2017, **50**, 1909–1918.
25 S. Broll, F. Nuebling, A. Luzio, D. Lentzas, H. Komber, M. Caironi and M. Sommer, *Macromolecules*, 2015, **48**, 7481–7488.
26 F. Lombeck, F. Marx, K. Strassel, S. Kunz, C. Lienert, H. Komber, R. Friend and M. Sommer, *Polym. Chem.*, 2017, **8**, 4738–4745.
27 N. S. Gobalasingham, J. E. Carle, F. C. Krebs, B. C. Thompson, E. Bundgaard and M. Helgesen, *Macromol. Rapid Commun.*, 2017, **38**, 1700526.
28 X. Gu, Y. Zhou, K. Gu, T. Kurosawa, Y. Guo, Y. Li, H. Lin, B. C. Schroeder, H. Yan, F. Molina-Lopez, C. J. Tassone, C. Wang, S. C. B. Mannsfeld, H. Yan, D. Zhao, M. F. Toney and Z. Bao, *Adv. Energy Mater.*, 2017, **7**, 1602742.
29 F. C. Krebs, S. A. Gevorgyan and J. Alstrup, *Journal of Materials Chemistry*, 2009, **19**, 5442.
30 F. C. Krebs, S. A. Gevorgyan, B. Gholamkhass, S. Holdcroft, C. Schlenker, M. E. Thompson, B. C. Thompson, D. Olson, D. S. Ginley, S. E. Shaheen, H. N. Alshareef, J. W. Murphy, W. J. Youngblood, N. C. Heston, J. R. Reynolds, S. Jia, D. Laird, S. M. Tuladhar, J. G. A. Dane, P. Atienzar, J. Nelson, J. M. Kroon, M. M. Wienk, R. A. J. Janssen, K. Tvingstedt, F. Zhang, M. Andersson, O. Inganaes, M. Lira-Cantu, R. de Bettignies, S. Guillerez, T. Aernouts, D. Cheyns, L. Lutsen, B. Zimmermann, U. Wuerfel, M. Niggemann, H.-F. Schleiermacher, P. Liska, M.

This journal is © The Royal Society of Chemistry 20xx

Please do not adjust margins

Graetzel, P. Lianos, E. A. Katz, W. Lohwasser and B. Jannon, *Sol. Energy Mater. Sol. Cells*, 2009, **93**, 1968–1977.
31 F. C. Krebs, *Solar Energy Materials and Solar Cells*, 2009, **93**, 394–412.
32 L. Yang, H. Zhou and W. You, *J. Phys. Chem. C*, 2010, **114**, 16793–16800.
33 K. R. Graham, C. Cabanetos, J. P. Jahnke, M. N. Idso, A. El Labban, G. O. Ngongang Ndjawa, T. Heumueller, K. Vandewal, A. Salleo, B. F. Chmelka, A. Amassian, P. M. Beaujuge and M. D. McGehee, *J. Am. Chem. Soc.*, 2014, **136**, 9608–9618.
34 I. Constantinou, T.-H. Lai, E. D. Klump, S. Goswami, K. S. Schanze and F. So, *ACS Appl. Mater. Interfaces*, 2015, **7**, 26999–27005.
35 M. Causa', J. De Jonghe-Risse, M. Scarongella, J. C. Brauer, E. Buchaca-Domingo, J.-E. Moser, N. Stingelin and N. Banerji, *Nature Communications*, 2016, **7**, 12556.
36 C. Zhang, S. Langner, A. V. Mumyatov, D. V. Anokhin, J. Min, J. D. Perea, K. L. Gerasimov, A. Osvet, D. A. Ivanov, P. Troshin, N. Li and C. J. Brabec, *J. Mater. Chem. A*, 2017, **5**, 17570–17579.
37 J. W. Jung, T. P. Russell and W. H. Jo, *ACS Appl. Mater. Interfaces*, 2015, **7**, 13666–13674.
38 S. Liu, X. Bao, W. Li, K. Wu, G. Xie, R. Yang and C. Yang, *Macromolecules*, 2015, **48**, 2948–2957.
39 Y. Zou, A. Najari, P. Berrouard, S. Beaupre, B. Reda Aich, Y. Tao and M. Leclerc, *J. Am. Chem. Soc.*, 2010, **132**, 5330–5331.
40 S. Beaupre, A. Pron, S. H. Drouin, A. Najari, L. G. Mercier, A. Robitaille and M. Leclerc, *Macromolecules*, 2012, **45**, 6906–6914.
41 H. Zheng, J. Wang, W. Chen, C. Gu, J. Ren, M. Qiu, R. Yang and M. Sun, *J. Mater. Chem. C*, 2016, **4**, 6280–6286.
42 M. S. Sarjadi and A. Iraqi, *Polymers & Polymer Composites*, 2016, **24**, 703–709.
43 R. Matsidik, H. Komber, A. Luzio, M. Caironi and M. Sommer, *J. Am. Chem. Soc.*, 2015, **137**, 6705–6711.
44 K. Yamazaki, J. Kuwabara and T. Kanbara, *Macromolecular Rapid Communications*, 2013, **34**, 69–73.
45 A. E. Rudenko, A. A. Latif and B. C. Thompson, *Nanotechnology*, 2014, **25**, 014005/1-014005/9, 9 pp.
46 J.-R. Pouliot, F. Grenier, J. T. Blaskovits, S. Beaupré and M. Leclerc, *Chem. Rev.*, 2016, **116**, 14225–14274.
47 E. Al-Naamani, A. Gopal, M. Ide, I. Osaka and A. Saeki, *ACS Appl. Mater. Interfaces*, 2017, **9**, 37702–37711.
48 S. Beaupre, S. Shaker-Sepasgozar, A. Najari and M. Leclerc, *J. Mater. Chem. A*, 2017, **5**, 6638–6647.
49 T. Vahlenkamp and G. Wegner, *Macromolecular Chemistry and Physics*, 1994, **195**, 1933–1952.
50 D. Schiefer, H. Komber, F. Mugwanga Keheze, S. Kunz, R. Hanselmann, G. Reiter and M. Sommer, *Macromolecules*, 2016, **49**, 7230–7237.
51 J. Huang, K. Wang, S. Gupta, G. Wang, C. Yang, S. H. Mushrif and M. Wang, *J. Polym. Sci. Part A: Polym. Chem.*, 2016, **54**, 2015–2031.
52 K. Wang, G. Wang and M. Wang, *Macromol. Rapid Commun.*, 2015, **36**, 2162–2170.
53 X. Wang and M. Wang, *Polym. Chem.*, 2014, **5**, 5784–5792.
54 K. Wang and M. Wang, *J. Polym. Sci. Part A: Polym. Chem.*, 2017, **55**, 1040–1047.
55 T. Erb, U. Zhokhavets, G. Gobsch, S. Raleva, B. Stühn, P. Schilinsky, C. Waldauf and C. J. Brabec, *Advanced Functional Materials*, 2005, **15**, 1193–1196.
56 Z. Xiao, K. Sun, J. Subbiah, T. Qin, S. Lu, B. Purushothaman, D. J. Jones, A. B. Holmes and W. W. H. Wong, *Polym. Chem.*, 2015, **6**, 2312–2318.
57 F. Liu, D. Chen, C. Wang, K. Luo, W. Gu, A. L. Briseno, J. W. P. Hsu and T. P. Russell, *ACS Appl. Mater. Interfaces*, 2014, **6**, 19876–19887.
58 C. Wang, C. J. Mueller, E. Gann, A. C. Y. Liu, M. Thelakkat and C. R. McNeill, *J. Mater. Chem. A*, 2016, **4**, 3477–3486.
59 B. C. Thompson and J. M. J. Frechet, *Angew. Chem., Int. Ed.*, 2008, **47**, 58–77.

Please do not adjust margins

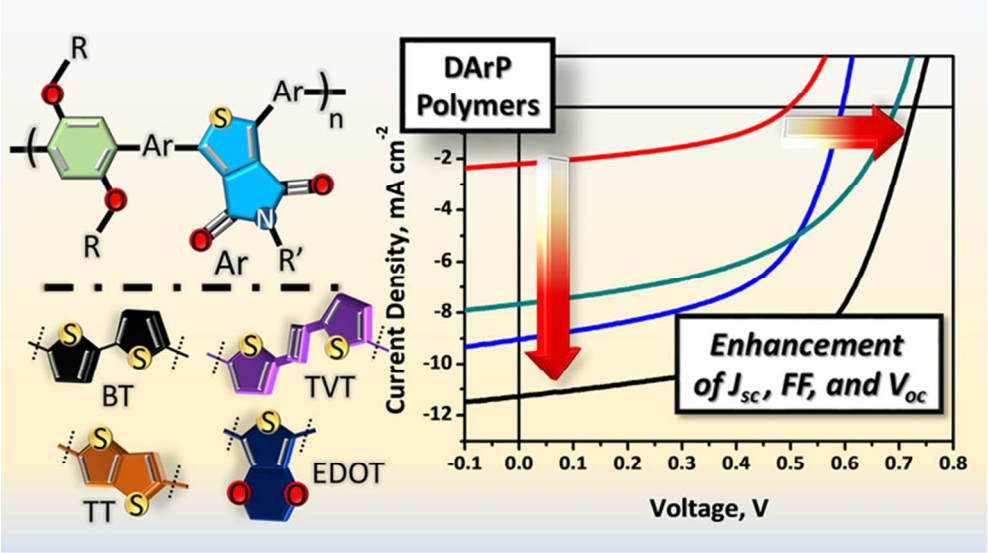

209x116mm (96 x 96 DPI)